Analysis of the *Streptococcus mutans* proteome during acid and oxidative stress reveals modules of co-expression and an expanded role for the TreR transcriptional regulator

Authors: Elizabeth L. Tinder[1,†], Roberta C. Faustoferri[2,†], Andrew A. Buckley[3], Robert G. Quivey, Jr.[2,4], Jonathon L. Baker[5,6*]

[1]Department of Infectious Disease, St. Jude Children's Research Hospital, Memphis, TN

[2]Center for Oral Biology, University of Rochester Medical Center, Rochester, NY

[3]Eshelman School of Pharmacy, University of North Carolina, Chapel Hill, NC

[4]Department of Microbiology & Immunology, University of Rochester Medical Center, Rochester, NY

[5]Genomic Medicine Group, J. Craig Venter Institute, La Jolla, CA

[6]Department of Pediatrics, UC San Diego School of Medicine, La Jolla, CA

[†]Authors contributed equally to this manuscript

*Corresponding author:

Jonathon L. Baker
Genomic Medicine Group
J. Craig Venter Institute
4120 Capricorn Lane
La Jolla, CA 9237

Running Title: Acid and oxidative stress proteomes of *S. mutans*

Keywords: *Streptococcus mutans*, proteome, oxidative stress, Nox, TreR

ORCIDs: ELT: 0000-0002-0262-5253, RCF: 0000-0002-5741-4971, JLB: 0000-0001-5378-322X

Abstract

Streptococcus mutans promotes a tooth-damaging dysbiosis in the oral microbiota because it can form biofilms and survive acid stress better than most of its ecological competitors, which are typically health-associated. Many of these commensals produce hydrogen peroxide, therefore *S. mutans* must manage both oxidative stress and acid stress with coordinated and complex physiological responses. In this study, the proteome of *S. mutans* was examined during regulated growth in acid and oxidative stresses, as well as in deletion mutants with impaired oxidative stress phenotypes, Δ*nox* and Δ*treR.* 607 proteins exhibited significantly different abundance levels across the conditions tested, and correlation network analysis identified modules of co-expressed proteins that were responsive to the deletion of *nox* and/or *treR,* as well as acid and oxidative stress. The data provided evidence explaining the ROS-sensitive and mutacin-deficient phenotypes exhibited by the Δ*treR* strain. SMU.1069-1070, a poorly understood LytTR system, had elevated abundance in the Δ*treR* strain. *S. mutans* LytTR systems regulate mutacin production and competence, which may explain how TreR affects mutacin production. Furthermore, the gene cluster that produces mutanobactin, a lipopeptide important in ROS tolerance, displayed reduced abundance in the Δ*treR* strain. The role of Nox as a keystone in the oxidative stress response was also emphasized. Crucially, this dataset provides oral health researchers with a proteome atlas that will enable a more complete understanding of the *S. mutans* stress responses that are required for pathogenesis, and facilitate the development of new and improved therapeutic approaches for dental caries.

48 **Importance**

49 Dental caries is the most common chronic infectious disease worldwide, and disproportionally
50 affects marginalized socioeconomic groups. *Streptococcus mutans* is a considered a primary
51 etiologic agent of caries, with its pathogenicity dependent on coordinated physiologic stress
52 responses that mitigate the damage caused by the oxidative and acid stress common within
53 dental plaque. In this study, the proteome of *S. mutans* was examined during growth in acidic
54 and oxidative stresses, as well in *nox* and *treR* deletion mutants. 607 proteins were differentially
55 expressed across the strains/growth conditions, and modules of co-expressed proteins were
56 identified, which enabled mapping the acid and oxidative stress responses across *S. mutans*
57 metabolism. The presence of TreR was linked to mutacin production via LytTR system signaling
58 and to oxidative stress via mutanobactin production. The data provided by this study will guide
59 future research elucidating *S. mutans* pathogenesis and developing improved preventative and
60 treatment modalities for dental caries.

61

Observation

Dental caries remains the most common chronic infectious disease worldwide, and is caused by a dysbiotic dental plaque microbiome that demineralizes tooth enamel via the fermentation of dietary carbohydrates to acid (1). *Streptococcus mutans* is considered a primary etiologic agent of caries due to its exceptional ability to facilitate biofilm formation when provided with sucrose, and its acidophilic niche (2). *S. mutans* employs a robust acid stress response that renders it more acid-tolerant than many of the health-associated commensals that it competes with ecologically. A number of these rival Streptococci produce H_2O_2, therefore *S. mutans* must also deal with oxidative stress (3, 4). Numerous studies have examined the role of various genes in these overlapping stress responses and the complex regulatory network that governs them. Previously, our research group identified that the NADH oxidase, Nox, was a linchpin of the *S. mutans* oxidative stress response at the intersection of two oxidative stress regulons (4). Furthermore, the transcriptional regulator of the trehalose utilization operon, TreR, had an unexpected role in oxidative stress and toxin production (5). In this study, mass spectrometry was used to elucidate changes in the *S. mutans* proteome during growth in acid or oxidative stresses, and upon deletion of *nox* or *treR.*

The archetype *S. mutans* strain, UA159 (6), along with the Δ*nox* and Δ*treR* mutant strains were analyzed during tightly-controlled steady-state growth conditions enabled by chemostats set at neutral pH (7), acidic pH (5) and/or sparged with air to maintain an 8.4% dissolved oxygen concentration (i.e. oxidative stress, as described in (4)). Text S1 contains a full description of the materials and methods used in this study. Liquid chromatography-tandem mass spectrometry was performed to examine the proteome of these strains and growth conditions. 1,384 unique proteins were detected across the 8 strains/growth conditions (Table S1). PCA analysis indicated three main clusters of samples: all pH 5 samples, regardless of oxidative stress or genotype; the pH 7 samples without oxidative stress (UA159 and Δ*treR*); and the pH 7 samples under oxidative stress (UA159 + air and Δ*nox*) (Figure 1A). The proteins that were the largest drivers in ordination

space towards the pH 5 samples were SpaP, GtfC, GtfD, SMU_63c, while GbpB and AdhE were associated with the pH 7 samples, and Pfl and AtlA were associated with the pH 7 samples under oxidative stress (Figure 1A). Differential expression analyses between pairwise strains/growth conditions is provided in File S1.

Correlation network analysis was performed to observe modules of co-expressed proteins under the various conditions (Figure 1B). This analysis revealed two large clusters of proteins associated with elevated abundance at either pH 5 or pH 7 (Figure 1D and H). Several smaller sub-clusters were associated with other discrete expression profiles such as oxidative stress or deletion of the TreR regulator (Figure 1CEFGIJK). A cluster associated with oxidative stress, either through addition of air or deletion of *nox,* included many of the well-established proteins of the oxidative stress tolerance response, including Tpx, GshR, Sod, SloR, and VicR (Figure 1K). An adjacent cluster of proteins, including the Adh operon, as well as Dpr, AlsS, and much of the purine biosynthesis gene cluster, had elevated abundance at pH 7 with air, but not in Δ*nox* (Figure 1C).

Intriguingly, two sub-clusters displayed expression profiles specifically affected by the presence of the TreR regulator. DivIC and MurD, involved in cell wall synthesis and cell division, as well as the autoregulatory LytTR system, SMU.1069-1070, had increased expression in the Δ*treR* strain (Figure 1E). SMU.1069-1070 exhibits crosstalk with the more well-characterized LytTR systems, HdrRM and BrsRM, known to regulate competence and bacteriocin production (7, 8). Since TreR and trehalose operon expression play a role in competence (9), and the production of mutacins IV, V, and VI (5), through unknown mechanisms, signaling through SMU.1069-1070 is an attractive hypothesis. Although the mutacin IV, V, and VI NRPS products themselves are too small to be detected by the proteomics analysis employed here, further evidence linking TreR to mutacin production was observed. Several proteins within mutacin biosynthetic gene clusters (BGCs) did have significantly decreased abundance in the Δ*treR* strain,

including CopYAZ (mutacin VI BGC) and SMU.1904 and SMU.1910 (mutacin V/CipB BGC) (File S1).

Meanwhile, the proteins from the trehalose operon itself, as well as the large mutanobactin BGC (SMU.1334-1349) were reduced in the Δ*treR* strain (Figure 1F). This further confirmed that in *S. mutans,* TreR serves as an activator of tre operon expression, rather than as a repressor, as seen in other species (5). Mutanobactin, a non-ribosomal lipopeptide, appears to have a role in helping *S. mutans* deal with oxidative stress (10). Therefore, it is possible that reduced abundance of the mutanobactin BGC may explain the impaired ROS tolerance in the Δ*treR* strain. Interestingly, Nox and TreR did not appear in the correlation network, likely due to their absence in deletion mutant strains obscuring correlations. In repeated correlation analysis with the deletion mutant samples removed, Nox expression was tightly-correlated with 33 co-expressed proteins, mainly from the clusters of genes associated with oxidative stress, further confirming its role as a keystone protein in the *S. mutans* oxidative stress response (Figure 2L). Contrarily, in the reanalysis, TreR only had one protein correlation with $\rho \geq 0.8$, SMU_690. Since TreR did not exhibit strong correlation with other proteins, but its absence had a major effect on the abundance of a number of proteins, it seems modulation of transcriptional regulatory activity for TreR, rather than just TreR expression level, is likely to be key in its role as a regulator.

Differential rankings (11) were utilized to determine the proteins most associated with acid and oxidative stress. KOs from the sub-clusters associated with pH 5 and pH 7 (Figures 1D and 1H) made up the majority of the proteins associated with the cognate pH (Figure 2A), while proteins from the sub-clusters associated with oxidative stress (Figures 1C and 1K) were in fact correlated with the associated growth condition, based on supervised methods (Figure 2B). To further examine the impact of the genotypes and growth conditions on *S. mutans* metabolism, proteins with associated KO numbers from the sub-clusters in Figure 1C-J were overlaid onto a map of the metabolism of *S. mutans* UA159 using KEGG Mapper (https://www.genome.jp/kegg/)

(Figure 2). Table S3 provides a table of KO numbers and colors to be used by the reader to generate an interactive version of the metabolic map shown in Figure 2C using KEGG Mapper Color. Many of the large-scale trends observed were in-line with previous, transcriptomic and proteomic observations (3, 12). These included increased abundance of proteins involved in fatty acid biosynthesis, the partial TCA cycle and pyrimidine metabolism at pH 7, and increased abundance of proteins involved in arginine deiminase, BCAA biosynthesis, purine metabolism, and the F_1F_0 ATPase at pH 5. Overall, this updated perspective of the *S. mutans* proteome provides a comprehensive interpretation of how this organism deals with acid and oxidative stress, permitting its key role in the dysbiosis that leads to caries pathogenesis. This study also highlights several principal avenues for future research, including the importance of the TreR regulator.

Data Availability

The raw mass spectrometry output files are available in the MassIVE Repository (massive.ucsd.edu) with the accession number MSV000088252.

Figure Legends

Figure 1: The proteome of *S. mutans* during acid and oxidative stress. (A) PCoA biplot of the Bray-Curtis dissimilarity between samples of the indicated strain and growth condition, represented by the colored spheres. Feature loadings (i.e. proteins driving distances in ordination space) are illustrated by the vectors, which are labeled with the cognate feature name and colored based on that feature's cluster in Panel B. **(B)** Clustering of *S. mutans* proteins into co-expression clusters. Protein association network illustrating co-expressed proteins. Prior to clustering, proteins were filtered for significant differences using an uncorrected ANOVA $p < 0.01$ (607 proteins). Correlations (edges) with a Spearman's $\rho > 0.8$ are shown and only positive correlations were considered. Edge width is representative of Spearman's ρ. Clusters were manually selected as indicated by the node color. **(C-K)** Sub-clusters are annotated with a heatmap indicating protein abundance across the 8 strains/growth conditions. Heatmap rows are clustered by Spearman's ρ. A version of the full network with each node labeled is available in Figure S1, and versions of the Acid Stress and Neutral pH heatmaps with each row labeled are available in Figure S2. A pairwise correlation table of all proteins is provided in Table S2. A heatmap illustrating expression of the 54 proteins that were differentially expressed based on ANOVA, but did not have significant correlations with other proteins, is provided in Figure S3. **(L)** Proteins that correlate with Nox when the Δ*nox* samples are not included in the network analyses. The Δ*nox* strain data likely obscured proteins that correlate with Nox, therefore the correlation network analysis was repeated without the Δ*nox* data. The network shown here is a sub-cluster of all 33 proteins significantly correlating with Nox expression. Nox is represented by the yellow diamond, all other nodes are colored by the sub-cluster determined in Figure 1B-K. Edge is representative of Spearman's ρ. Only positive correlations with $\rho > 0.8$ are shown.

Figure 2: Metabolic modules of the *S. mutans* acid and oxidative stress responses. (A) Differential ranking of proteins associated with pH 5 vs pH 7. Songbird was used to rank proteins with respect to pH, and Qurro (13) was used to visualize the resulting ranks (only the top and bottom 150 proteins are shown). Proteins with known KOs in the sub-clusters shown in Figures 1D and 1H are highlighted in orange and dark green, respectively. **(B)** Differential ranking of proteins associated with high O_2 (UA159 + air and Δ*nox*) vs. low O_2 (UA159 and Δ*treR*). Songbird was used to rank proteins with respect to high vs low O_2, and Qurro (13) was used to visualize the resulting ranks (only the top and bottom 150 proteins are shown). Proteins with known KOs in the sub-clusters shown in Figures 1C and 1K are highlighted in yellow and light green, respectively. **(C)** Metabolism of *S. mutans* during acid and oxidative stress. All proteins from the sub-clusters shown in Figure 1C-K with known KOs were overlaid on to a map of the known metabolism of *S. mutans* using KEGG Mapper (https://www.genome.jp/kegg). Colors of each sub-cluster from Figure 1 are maintained, as described in the Key.

Supplemental Figure and File Legends

Figure S1: Correlation network of the *S. mutans* proteome. The complete Figure 1B network, with each node is labeled with the cognate protein name. Clustering of *S. mutans* proteins into co-expression clusters. Protein association network illustrating co-expressed proteins. Prior to clustering, proteins were filtered for significant differences using an uncorrected ANOVA $p < 0.01$ (607 proteins). Correlations (edges) with a Spearman's $\rho > 0.8$ are shown and only positive correlations were considered. Edge width is representative of Spearman's ρ. Clusters were manually selected as indicated by the node color.

Figure S2: Expression profiles of proteins associated with pH 5 (A) or pH 7 (B). These are expanded versions of the heatmaps appearing in Figure 1 panels D and H, with each row labeled. Rows are clustered by Spearman's ρ.

Figure S3: Expression profile of differentially-expressed genes that had no significant correlations. Heatmap showing the expression of proteins that made the differential expression ANOVA $p \geq 0.5$ cutoff, but did not have any correlations with other proteins with a Spearman's $\rho \geq 0.8$. Rows are clustered by Spearman's ρ.

Table S1: Normalized abundances of detected proteins

Table S2: Spearman's Rank correlations between differentially-expressed proteins.

Table S3: KO and color list to generate interactive *S. mutans* metabolism map using KEGG Mapper – Color (https://www.genome.jp/kegg/mapper/color.html)

File S1: Excel file containing pairwise $\log_2$ fold-changes and p-values for each protein between all 8 strain/growth conditions

Text S1: Supplemental Materials and Methods

Acknowledgements

The authors thank Kevin Welle and the Mass Spectrometry Resource Lab at the University of Rochester Medical Center for performing the proteomics analysis. This study was supported by NIH/NIDCR grants R01-DE013683 (R.G.Q.) and K99-DE029228 (J.L.B.).

References

1. Pitts NB, Zero DT, Marsh PD, Ekstrand K, Weintraub JA, Ramos-Gomez F, Tagami J, Twetman S, Tsakos G, Ismail A. 2017. Dental caries. Nat Rev Dis Primers 3:17030.
2. Lemos JA, Palmer SR, Zeng L, Wen ZT, Kajfasz JK, Freires IA, Abranches J, Brady LJ. 2019. The Biology of *Streptococcus mutans*. Microbiol Spectr 7.
3. Baker JL, Faustoferri RC, Quivey RG, Jr. 2017. Acid-adaptive mechanisms of *Streptococcus mutans*-the more we know, the more we don't. Mol Oral Microbiol 32:107-117.
4. Baker JL, Derr AM, Karuppaiah K, MacGilvray ME, Kajfasz JK, Faustoferri RC, Rivera-Ramos I, Bitoun JP, Lemos JA, Wen ZT, Quivey RG, Jr. 2014. *Streptococcus mutans* NADH oxidase lies at the intersection of overlapping regulons controlled by oxygen and NAD^+ levels. J Bacteriol 196:2166-77.
5. Baker JL, Lindsay EL, Faustoferri RC, To TT, Hendrickson EL, He X, Shi W, McLean JS, Quivey RG, Jr. 2018. Characterization of the trehalose utilization operon in *Streptococcus mutans* reveals that the TreR transcriptional regulator is involved in stress response pathways and toxin production. J Bacteriol 200.
6. Ajdic D, McShan WM, McLaughlin RE, Savic G, Chang J, Carson MB, Primeaux C, Tian R, Kenton S, Jia H, Lin S, Qian Y, Li S, Zhu H, Najar F, Lai H, White J, Roe BA, Ferretti JJ. 2002. Genome sequence of *Streptococcus mutans* UA159, a cariogenic dental pathogen. Proc Natl Acad Sci U S A 99:14434-9.
7. Zou Z, Qin H, Brenner AE, Raghavan R, Millar JA, Gu Q, Xie Z, Kreth J, Merritt J. 2018. LytTR Regulatory Systems: A potential new class of prokaryotic sensory system. PLoS Genet 14:e1007709.
8. Xie Z, Okinaga T, Niu G, Qi F, Merritt J. 2010. Identification of a novel bacteriocin regulatory system in *Streptococcus mutans*. Mol Microbiol 78:1431-47.
9. Underhill SAM, Shields RC, Burne RA, Hagen SJ. 2019. Carbohydrate and PepO control bimodality in competence development by *Streptococcus mutans*. Mol Microbiol 112:1388-1402.
10. Wu C, Cichewicz R, Li Y, Liu J, Roe B, Ferretti J, Merritt J, Qi F. 2010. Genomic island TnSmu2 of *Streptococcus mutans* harbors a nonribosomal peptide synthetase-polyketide synthase gene cluster responsible for the biosynthesis of pigments involved in oxygen and H_2O_2 tolerance. Appl Environ Microbiol 76:5815-26.
11. Morton JT, Marotz C, Washburne A, Silverman J, Zaramela LS, Edlund A, Zengler K, Knight R. 2019. Establishing microbial composition measurement standards with reference frames. Nat Commun 10:2719.
12. Len ACL, Harty DWS, Jacques NA. 2004. Proteome analysis of *Streptococcus mutans* metabolic phenotype during acid tolerance. Microbiology (Reading) 150:1353-1366.
13. Fedarko MW, Martino C, Morton JT, Gonzalez A, Rahman G, Marotz CA, Minich JJ, Allen EE, Knight R. 2020. Visualizing 'omic feature rankings and log-ratios using Qurro. NAR Genom Bioinform 2:lqaa023.

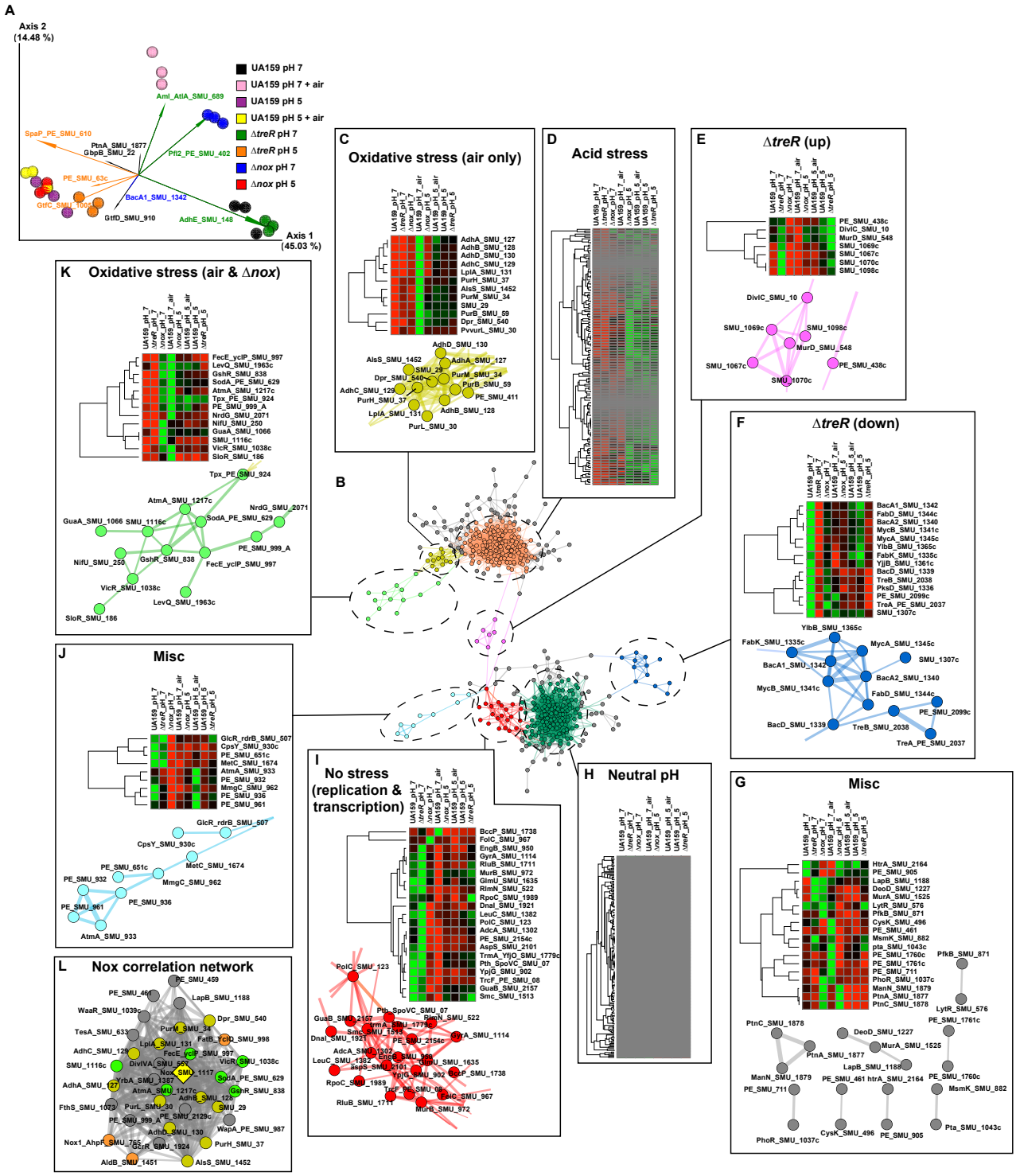
A
Axis 2
(14.48 %)
Axis 1
(45.03 %)
UA159 pH 7
UA159 pH 7 + air
UA159 pH 5
UA159 pH 5 + air
ΔtreR pH 7
ΔtreR pH 5
Δnox pH 7
Δnox pH 5
AmI_AtlA_SMU_689
SpaP_PE_SMU_610
PtnA_SMU_1877
GbpB_SMU_22
Pfl2_PE_SMU_402
PE_SMU_63c
BacA1_SMU_1342
GtfC_SMU_1009
GtfD_SMU_910
AdhE_SMU_148
B
C
Oxidative stress (air only)
AdhA_SMU_127
AdhB_SMU_128
AdhD_SMU_130
AdhC_SMU_129
LplA_SMU_131
PurH_SMU_37
AlsS_SMU_1452
PurM_SMU_34
SMU_29
PurB_SMU_59
Dpr_SMU_540
PvvurL_SMU_30
D
Acid stress
E
ΔtreR (up)
PE_SMU_438c
DivIC_SMU_10
MurD_SMU_548
SMU_1069c
SMU_1067c
SMU_1070c
SMU_1098c
F
ΔtreR (down)
BacA1_SMU_1342
FabD_SMU_1344c
BacA2_SMU_1340
MycB_SMU_1341c
MycA_SMU_1345c
YlbB_SMU_1365c
FabK_SMU_1335c
YjjB_SMU_1361c
BacD_SMU_1339
TreB_SMU_2038
PksD_SMU_1336
PE_SMU_2099c
TreA_PE_SMU_2037
SMU_1307c
G
Misc
HtrA_SMU_2164
PE_SMU_905
LapB_SMU_1188
DeoD_SMU_1227
MurA_SMU_1525
LytR_SMU_576
PfkB_SMU_871
CysK_SMU_496
PE_SMU_461
MsmK_SMU_882
pta_SMU_1043c
PE_SMU_1760c
PE_SMU_1761c
PE_SMU_711
PhoR_SMU_1037c
ManN_SMU_1879
PtnA_SMU_1877
PtnC_SMU_1878
H
Neutral pH
I
No stress
(replication &
transcription)
BccP_SMU_1738
PolC_SMU_967
EngB_SMU_950
GyrA_SMU_1114
RluB_SMU_1711
MurB_SMU_972
GlmU_SMU_1635
RlmN_SMU_522
RpoC_SMU_1989
DnaI_SMU_1921
LeuC_SMU_1382
PolC_SMU_123
AdcA_SMU_1302
PE_SMU_2154c
AspS_SMU_2101
TrmA_YfjO_SMU_1779c
Pth_SpoVC_SMU_07
YpjG_SMU_902
TrcF_PE_SMU_08
GuaB_SMU_2157
Smc_SMU_1513
J
Misc
GlcR_rdrB_SMU_507
CpsY_SMU_930c
PE_SMU_651c
MetC_SMU_1674
AtmA_SMU_933
PE_SMU_932
MmgC_SMU_962
PE_SMU_936
PE_SMU_961
K
Oxidative stress (air & Δnox)
FecE_yclP_SMU_997
LevQ_SMU_1963c
GshR_SMU_838
SodA_PE_SMU_629
AtmA_SMU_1217c
Tpx_PE_SMU_924
PE_SMU_999_A
NrdG_SMU_2071
NifU_SMU_250
GuaA_SMU_1066
SMU_1116c
VicR_SMU_1038c
SloR_SMU_186
L
Nox correlation network
PE_SMU_459
PE_SMU_461
LapB_SMU_1188
WaaR_SMU_1039c
Dpr_SMU_540
TesA_SMU_633
PurM_SMU_34
FatB_CHD_SMU_998
LplA_SMU_131
AdhC_SMU_129
FecE_yclP_SMU_997
SMU_1116c
DivIVA_SMU_9
VicR_SMU_1038c
Nox_SMU_1117
SodA_PE_SMU_629
YfbA_SMU_1387
AdhA_SMU_127
AtmA_SMU_1217c
GshR_SMU_838
AdhB_SMU_128
FthS_SMU_1023
PurL_SMU_30
SMU_29
PE_SMU_2129c
PE_SMU_999_A
WapA_PE_SMU_987
AdhD_SMU_130
Nox1_AhpF_SMU_785
GlcR_SMU_1924
PurH_SMU_37
AldB_SMU_1451
AlsS_SMU_1452

Figure 2

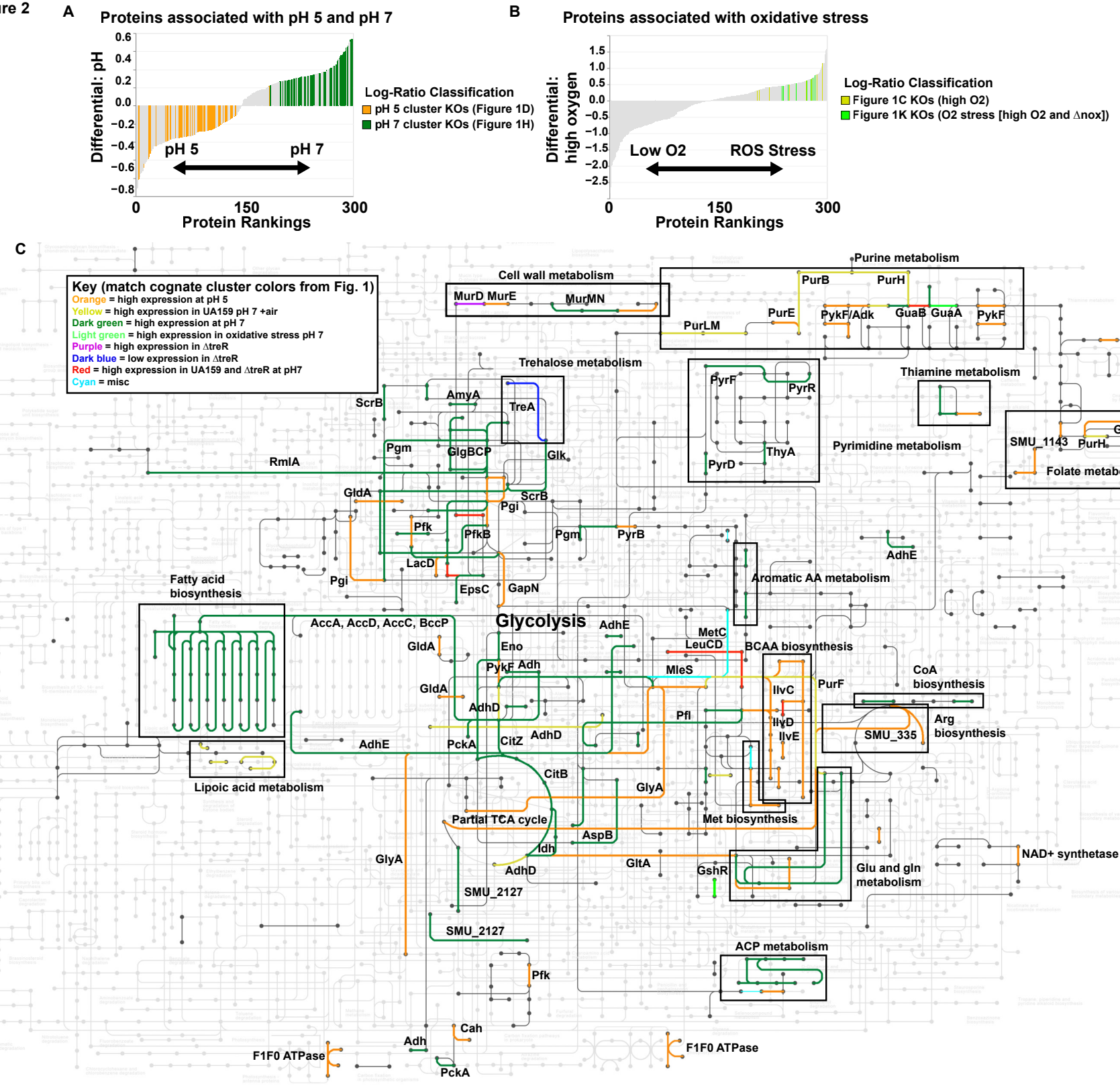
A
Proteins associated with pH 5 and pH 7
Differential: pH
0.6
0.4
0.2
0.0
−0.2
−0.4
−0.6
−0.8
pH 5
pH 7
0
150
300
Protein Rankings
Log-Ratio Classification
pH 5 cluster KOs (Figure 1D)
pH 7 cluster KOs (Figure 1H)
B
Proteins associated with oxidative stress
Differential: high oxygen
1.5
1.0
0.5
0.0
−0.5
−1.0
−1.5
−2.0
−2.5
Low O2
ROS Stress
0
150
300
Protein Rankings
Log-Ratio Classification
Figure 1C KOs (high O2)
Figure 1K KOs (O2 stress [high O2 and ΔnoxR])
C
Key (match cognate cluster colors from Fig. 1)
Orange = high expression at pH 5
Yellow = high expression in UA159 pH 7 +air
Dark green = high expression at pH 7
Light green = high expression in oxidative stress pH 7
Purple = high expression in ΔtreR
Dark blue = low expression in ΔtreR
Red = high expression in UA159 and ΔtreR at pH7
Cyan = misc
Cell wall metabolism
MurD MurE
MurMN
Purine metabolism
PurB
PurH
PurE
PykF/Adk
GuaB GuaA
PykF
PurLM
Trehalose metabolism
AmyA
TreA
ScrB
Pgm
GlgBCP
Glk
RmlA
GldA
ScrB
Pgi
Pfk
PfkB
Pgm
PyrB
LacD
Pgi
EpsC
GapN
PyrF
PyrR
ThyA
PyrD
Thiamine metabolism
Pyrimidine metabolism
GlyA
SMU_1143
PurH
Folate metabolism
AdhE
Aromatic AA metabolism
Fatty acid biosynthesis
AccA, AccD, AccC, BccP
Glycolysis
AdhE
GldA
Eno
PykF
Adh
GldA
AdhD
AdhE
PckA
CitZ
AdhD
CitB
GlyA
Partial TCA cycle
AspB
Idh
GlyA
AdhD
GltA
SMU_2127
SMU_2127
Lipoic acid metabolism
MetC
LeuCD
BCAA biosynthesis
MleS
Pfl
IlvC
IlvD
IlvE
PurF
CoA biosynthesis
SMU_335
Arg biosynthesis
Met biosynthesis
GshR
Glu and gln metabolism
NAD+ synthetase
ACP metabolism
Pfk
Cah
Adh
PckA
F1F0 ATPase
F1F0 ATPase